

Ref. 11 yields the dot-dashed line in Fig. 3b). The predicted Z dependence shows the opposite trend of the measured Z dependence – it decreases monotonically with increasing Z . This trend indicates that the initial kinetic energy of the neck fragment exceeds the minimum required by the uncertainty relation. If we fix the initial energy of the neck fragment at 4 MeV, the dependence of $\langle E \rangle$ on Z is in approximate agreement with the experimental data, as shown in Fig. 3b) (dashed line). We also explored fixing the initial velocity of the neck fragment ($v=1.39$ cm/ns). The resulting dependence of $\langle E \rangle$ on Z (dotted line) is in reasonable agreement with the ^{252}Cf data but significantly overpredicts the present experimental data, particularly for the heavier IMFs. Reasonable agreement with the present experimental data is achieved in a constant-velocity scenario if an initial velocity of 0.77 cm/ns is assumed (solid line).

‡ Present address: Department of Chemistry, Purdue University, West Lafayette, IN

† Present address: Pathologists Associated, 2401 West University Ave., Muncie, IN 47302

1. D.E. Fields *et al.*, Phys. Rev. Lett. **69**, 3713 (1992).
2. Z. Fraenkel and S.G. Thompson, Phys. Rev. Lett., **14**, 438 (1964).
3. W.W. Wilcke *et al.*, Phys. Rev. Lett. **51**, 99 (1983).
4. R. Lacey *et al.*, Phys. Rev. C **37**, 2540 (1988).
5. K. Siwek-Wilczynska *et al.*, Phys. Rev. C **48**, 228 (1993).
6. H. Ikezoe *et al.*, Phys. Rev. C **49**, 968 (1994).
7. M. Fatyga, Ph.D. thesis, Indiana University, (1987).
8. S.W. Cosper, J. Cerny, and R.C. Gatti, Phys. Rev. **154**, 1193 (1967).
9. D.E. Fields, Ph.D. thesis, Indiana University (1992).
10. S.L. Whetstone, Jr. and T.D. Thomas, Phys. Rev. **154**, 1174 (1962).
11. I. Halpern, Physics and Chemistry of Fission, International Atomic Energy Agency, Vienna, 1965, vol. 2 p. 369.
12. Y. Boneh *et al.*, Phys. Rev. **156**, 1305 (1967).

EXCLUSIVE STUDIES OF CHARGED-PARTICLE EMISSION IN
 ^1H - and ^3He -INDUCED REACTIONS ON HEAVY NUCLEI

D.S. Ginger, E. Cornell, W.-C. Hsi, K. Kwiatkowski, R.T. de Souza,
 V.E. Viola, G. Wang, and N.R. Yoder
Indiana University Cyclotron Facility, Bloomington, Indiana 47408

R.G. Korteling
Simon Fraser University, Burnaby, British Columbia, Canada V5A 1S6

Nonequilibrium and equilibrium mechanisms of complex fragment emission have been investigated in the Fermi-energy/pion-threshold regime with the ISIS 4π detector array.

Beams of 200-MeV protons and 130- and 270-MeV ^3He from IUCF were incident on targets of ^{27}Al , $^{\text{nat}}\text{Ag}$ and ^{197}Au . These measurements constitute the first studies at these bombarding energies in which charged particles were detected with large solid-angle coverage, broad dynamic range and energy acceptance, and high granularity. Spectra of H and He isotopes and IMFs up to $Z \sim 15$ were measured over the energy interval $0.7 \leq E/A \leq 96$ MeV and angular range $14^\circ - 86.5^\circ$ and $93.5^\circ - 166^\circ$. The multiplicity trigger for event acceptance was set for valid signals in two or more of the 162 silicon detectors.

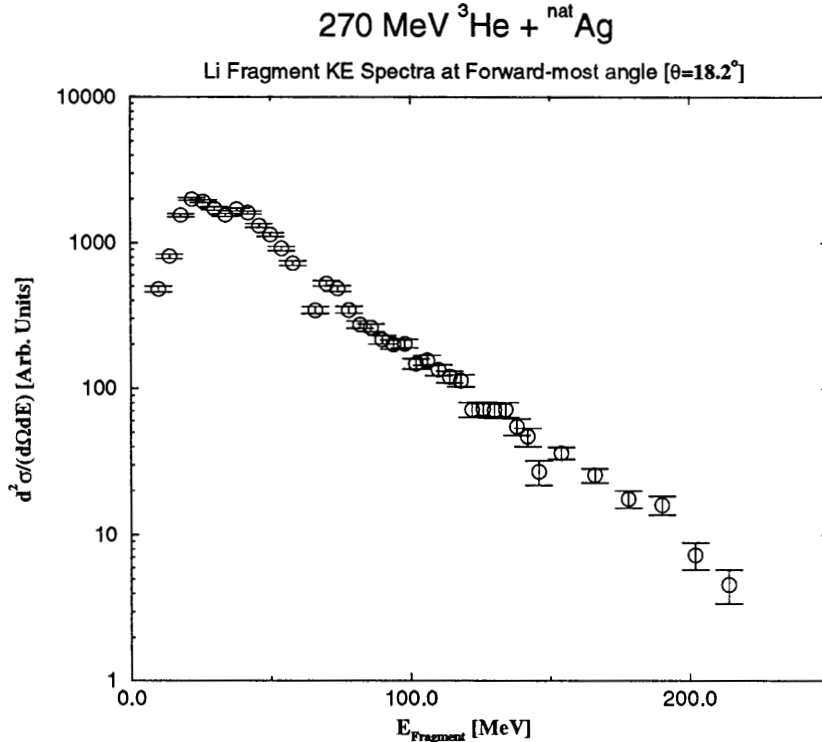


Figure 1. Energy spectrum of Li fragments measured at 18° in the 270-MeV $^3\text{He} + ^{\text{nat}}\text{Ag}$ reaction.

In Fig. 1, the spectrum of Li fragments is shown for fragments observed at $\langle\Theta\rangle = 18^\circ$ in the 270-MeV $^3\text{He} + ^{\text{nat}}\text{Ag}$ reaction. The data illustrate both the equilibrium component at low fragment energies and the hard exponential tail characteristic of nonequilibrium emission at higher energies.¹ Fragment kinetic energies are observed that approach the total available energy, corresponding to momenta about 30% greater than the beam momentum. Examination of the isotope-identified spectra above 50 MeV indicates that neutron-deficient ^6Li becomes increasingly dominant as the fragment energy increases, increasing from a ratio of $^6\text{Li}/^7\text{Li} = 1$ at 50-MeV to a value of 2.0 at 220-MeV fragment energy.

The angular distributions also indicate the equilibrium/nonequilibrium character of these reactions. Forward peaking of the fragment yields is evident and is strongly influenced by the energetic tails of the forward-angle spectra. In contrast, the yields in the backward hemisphere are approximately isotropic. Both this fact and the character of the backward-angle spectra support emission from an equilibrated source for these fragments.²

Charged-particle multiplicity (N_{CP}) probability distributions measured in these studies are presented in Fig. 2, where $\sum N_i/N_{\text{total}} = 1$. In the left-hand frame, the three

projectile-bombarding energy combinations incident on the ^{nat}Ag target are compared. The distributions scale systematically with beam energy, reaching maximum values of nine charged particles at the highest energy. The right-hand frame of Fig. 2 compares the charged-particle multiplicities for 270-MeV ^3He incident on ^{nat}Ag and ^{197}Au targets. The higher multiplicities observed for the ^{nat}Ag target reflect two factors: (1) neutron emission competes more favorably with charged particles in the de-excitation of heavy nuclei, and (2) higher temperatures (E^*/A_{residue}) are reached with the ^{nat}Ag target relative to ^{197}Au . The latter factor reduces the influence of the Coulomb barrier in inhibiting charged-particle decay.

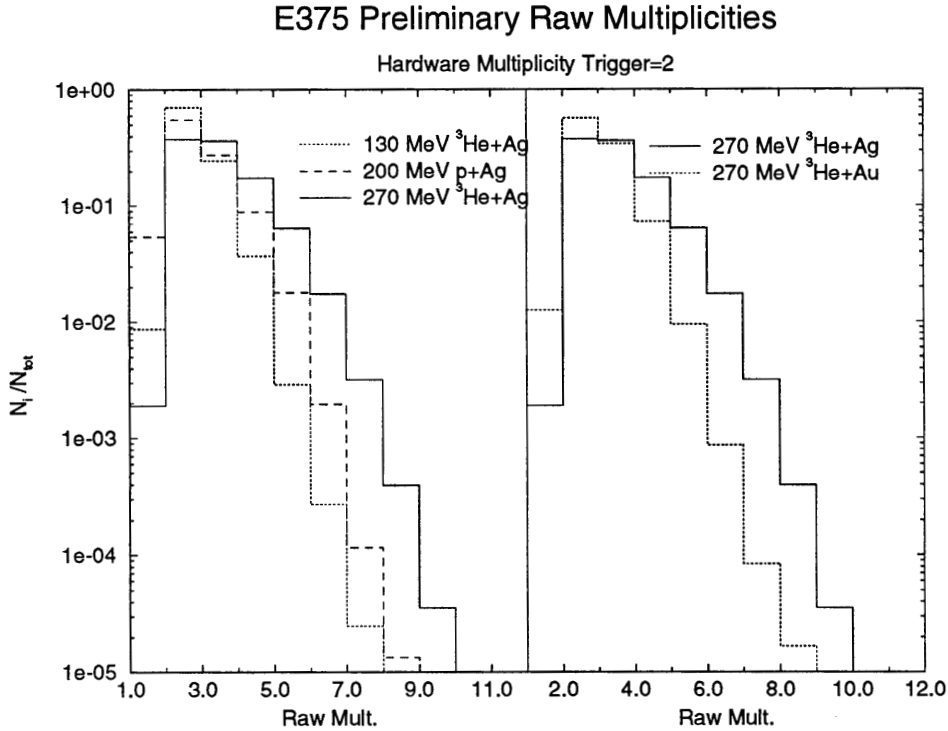


Figure 2. Probability distribution for the multiplicity of charged particles observed in: left frame – reactions on ^{nat}Ag , as indicated on figure, and right frame – comparison for Ag and ^{197}Au targets bombarded by 270-MeV ^3He .

To understand the relationship between the charged-particle multiplicity and IMF formation, in Fig. 3 we have plotted the total multiplicity probability distributions gated on three conditions: (1) events with at least one IMF, in which equilibrated events are a major component; (2) events with predominantly nonequilibrium IMFs, gated on Li fragments with kinetic energies above 90 MeV ($\sim 85\%$ of beam momentum), and (3) all events, primarily H and He isotopes. It is observed that by requiring one IMF in an event, we select a distribution skewed toward higher multiplicities. Since the number of charged particles should be a good gauge of excitation energy in these reactions, this result indicates that IMF emission originates from hotter sources than the average event.³ When nonequilibrium Li fragments are selected, the number of associated charged particles decreases by an order of magnitude for high N_{CP} . This reflects the energy carried away

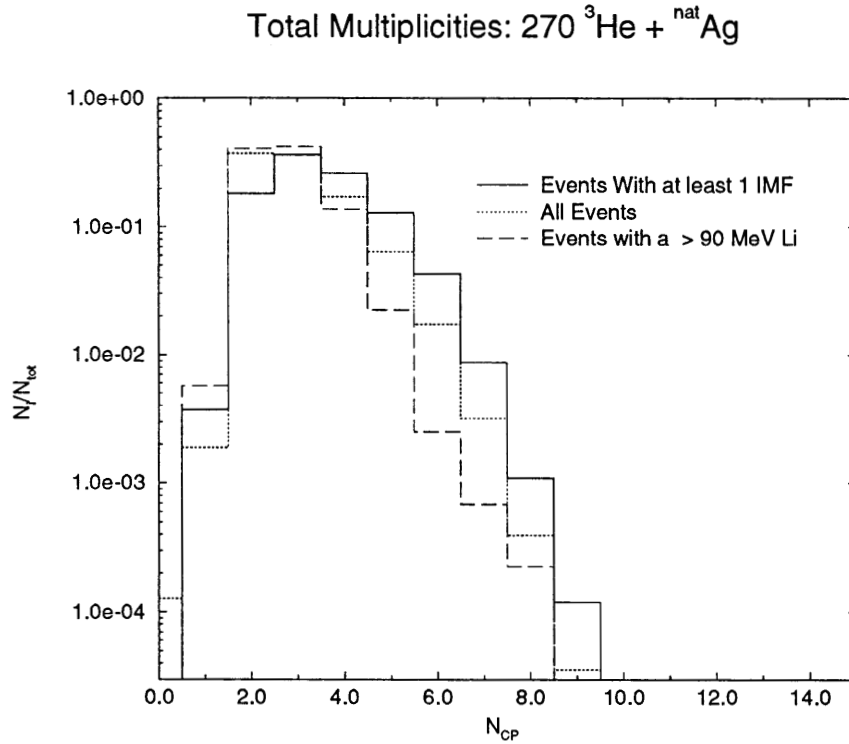


Figure 3. Comparison of charged particle multiplicity distributions for 270-MeV $^3\text{He} + \text{}^{\text{nat}}\text{Ag}$, reaction, gated on events with one IMF, all events and events with a Li fragment with energy ≥ 90 MeV, as indicated on figure.

from the system by these fast processes, leaving a cooler residue with decreased probability for emitting charged particles.

1. J. Wu *et al.*, Phys. Rev. C **19**, 370 (1978); *ibid.* 659; *ibid.* 698.
2. K. Kwiatkowski *et al.*, Phys. Lett. **B171**, 41 (1986).
3. W. Skulski *et al.*, Phys. Rev. C **40**, 1279 (1989).